

Supercell Tornadogenesis: Recent Progress in our State of Understanding

Jannick Fischer,^a Johannes M. L. Dahl,^a Brice E. Coffer,^b Jana Lesak House,^c

Paul M. Markowski,^d Matthew D. Parker,^b Christopher C. Weiss,^a Alex Schueth^a

^a Department of Geosciences, Texas Tech University, Lubbock, Texas

^b Department of Marine, Earth, and Atmospheric Sciences, North Carolina State University, Raleigh, North Carolina

^c Department of Geography, The Ohio State University, Columbus, Ohio

^d Department of Meteorology and Atmospheric Science, The Pennsylvania State University, University Park, Pennsylvania

Corresponding author: Jannick Fischer, jannick.fischer@kit.edu

Fischer's current affiliation: Karlsruhe Institute of Technology (KIT), Karlsruhe, Germany

Early Online Release: This preliminary version has been accepted for publication in *Bulletin of the American Meteorological Society*, may be fully cited, and has been assigned DOI 10.1175/BAMS-D-23-0031.1. The final typeset copyedited article will replace the EOR at the above DOI when it is published.

© 2024 American Meteorological Society. This is an Author Accepted Manuscript distributed under the terms of the default AMS reuse license. For information regarding reuse and general copyright information, consult the AMS Copyright Policy (www.ametsoc.org/PUBSReuseLicenses).

ABSTRACT: Over the last decade, supercell simulations and observations with ever increasing resolution have provided new insights into the vortex-scale processes of tornado formation. This article incorporates these and other recent findings into the existing three-step model by adding an additional fourth stage. The goal is to provide an updated and clear picture of the physical processes occurring during tornadogenesis. Specifically, we emphasize the importance of the low-level wind shear and mesocyclone for tornado potential, the organization and interaction of relatively small-scale pre-tornadic vertical vorticity maxima, and the transition to a tornado-characteristic flow. Based on these insights, guiding research questions are formulated for the decade ahead.

SIGNIFICANCE STATEMENT: This article provides a non-technical overview of how tornadoes form. Sequentially, the most important processes include the initial creation of rotating updrafts, the development of disorganized patches of rotation at the surface, the organization of these patches into a more defined, symmetric vortex, and the final transition into a fully developed tornado in which air turns abruptly upward very near the surface. Based on this proposed conceptual model, guiding research questions are formulated for the decade ahead.

CAPSULE: This article proposes an update on our understanding of how tornadoes form with a focus on the small-scale processes in recent high-resolution simulations and observations.

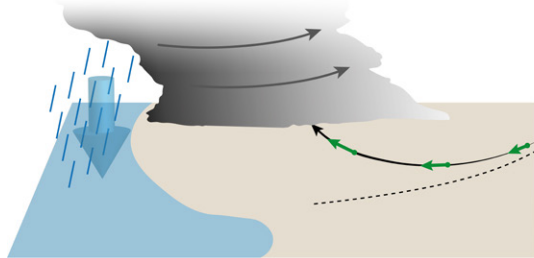
How does a tornado form? This is perhaps one of the most elementary yet enduring questions in meteorology. Even though severe-storms research has focused on this problem for over half a century, a lot of misleading information exists both within the community and the general public, including the “clash of warm and cold air” (Schultz et al. 2014) or the myth that storm-scale rotation simply descends to the surface to make a tornado. The purpose of this article is to lay out the currently evolving understanding of the physical processes in a non-technical format. Although many of the elements discussed herein apply to all types of tornadoes, we focus on those forming in supercells (Browning 1962; Doswell and Burgess 1993; Rotunno 1993) because they have the largest impact (Brotzge et al. 2013; Anderson-Frey and Brooks 2019). Supercells are “well-organized, monolithic units of vigorous long-lasting convection. A classic supercell in its mature stage consists of a rotating updraft [...] and a downdraft that coexists symbiotically with the updraft in an almost steady state” (Davies-Jones 2015, page 274). For a broader perspective on tornadoes and tornadic storms we refer the reader to Markowski and Richardson (2010, chapter 10).

The most established conceptual model of how a supercell tornado forms is described by Davies-Jones (2015) and includes three stages: generation of updraft rotation, generation of rotation at the ground, and concentration of that rotation leading to tornado formation. Research in recent years has revealed a high level of detail in the third stage (tornado formation). We account for this by splitting this stage into two, proposing an updated 4-step conceptual model. In the following sections, we guide the reader through these four stages. Since most of the recent findings are largely based on numerical simulations, we also discuss where observations of real supercells agree or disagree and what research is most needed.

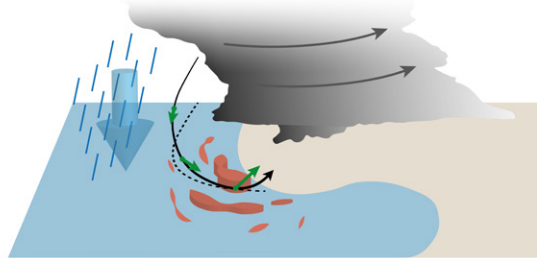
Stage 1: Mesocyclonic Rotation

The first stage of the supercell tornadogenesis process is necessarily the development of a rotating updraft, and with that a supercell’s defining feature: the *mesocyclone*. How an updraft acquires this mesocyclonic rotation is far-and-away the most well-understood component of the multi-step tornadogenesis process. Seminal work by Rotunno (1981), Lilly (1982) and Davies-Jones (1984) showed how horizontal vorticity (rotation along a horizontal axis, see green vectors in Fig. 1a), associated with the environmental vertical wind shear, is tilted into the vertical by the

(a) **Mesocyclonic Rotation**



(b) **Surface-level Rotation**



(c) **Organization & Stretching**



(d) **Transition to Tornado**

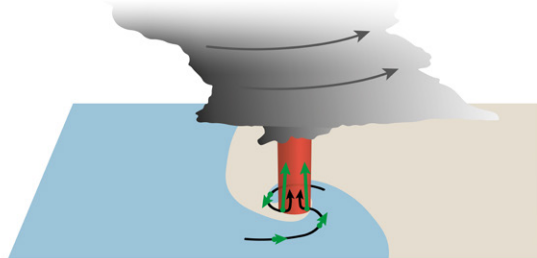


FIG. 1. The stages of tornado formation referred to in the text. The view is from the rear flank of the supercell (typically the western flank). The lowest few kilometers of the cloud surface are shaded gray, and the cold pool is shaded blue. Thin black arrows indicate parcel trajectories, thin gray arrows the low-level mesocyclone, and green vectors the direction and magnitude of vorticity, i.e., the axis and intensity of local rotation. Areas with relatively large vertical vorticity are shaded in red. The thick blue arrow indicates the downdraft referred to in the text on Stages 1 and 2, and the thick gray arrow the vertical (pressure-gradient) acceleration important in Stage 3.

supercell's updraft. For the updraft to rotate as a whole, the tilting of horizontal vorticity, with the local rotation axis closely aligned with the storm-relative inflow winds (referred to as streamwise vorticity; Davies-Jones 1984), as well as the conversion between curvature vorticity and shear vorticity (Dahl 2017), are essential.

The mesocyclone is critical for tornadogenesis mainly because the updraft's rotation is accompanied by a pressure deficit, which results in a pressure gradient that drives persistent upward accelerations below the level of free convection, where buoyancy is still neutral or negative (Coffer and Parker 2018; Goldacker and Parker 2021). This *dynamic* acceleration is not observed in other types of thunderstorms lacking a mesocyclone (e.g., Weisman and Klemp 1984) and is crucial

for tornadogenesis through stretching of vertical vorticity near the surface, as will be explained in Stage 3.

The development of mesocyclonic rotation throughout the depth of the supercell does not happen uniformly, however. Rotation at low altitudes within the storm, near the cloud base (roughly ~ 1 km above the surface) often intensifies later in the storm's lifecycle. This stronger rotation, sometimes referred to as the low-level mesocyclone, shows especially strong association with tornado potential and damage (Thompson et al. 2017). Environments that favor tornadoes, especially significant tornadoes, are known to possess strong vertical wind shear in the lower troposphere, based on both observed soundings (Rasmussen 2003; Craven and Brooks 2004) and model analyses (Markowski et al. 2003; Thompson et al. 2012). When this large ambient horizontal vorticity is ingested into a supercell's updraft (Fig. 1a), the low-level mesocyclone is characterized by intense and persistent dynamic lifting at and below cloud base (Markowski and Richardson 2014; Coffer et al. 2017; Peters et al. 2023). Low-level mesocyclones appear to source almost their entire inflow from very close to the ground (the lowest 500 - 1000 m; Coffer et al. 2023). This is likely why recent model analyses suggest that large horizontal, streamwise vorticity in the lowest few hundred meters above the surface may further favor tornado production (Parker 2014; Coffer et al. 2019, 2020; Nixon and Allen 2022), although some studies using observed soundings emphasize the importance of deeper layers of the wind profile (Coniglio and Parker 2020) and is discussed further in the summary.

Other sources of augmentation to the horizontal vorticity field can also enhance the strength of the low-level mesocyclone in the same way as ambient environmental vorticity, although their roles are still somewhat unclear. This includes surface roughness (Roberts and Xue 2017) as well as horizontal buoyancy gradients (baroclinity) along the forward flank (Klemp and Rotunno 1983; Rotunno and Klemp 1985; Markowski et al. 2012; Weiss et al. 2015). One such augmentation of current interest is the streamwise vorticity current (SVC; Orf et al. 2017), which will be described further below. Regardless of these potential augmentations to the low-level mesocyclone, a preponderance of evidence suggests environmental streamwise vorticity from winds that strongly veer and strengthen with height in the lower troposphere, perhaps even within the lowest few hundred meters, establishes a baseline probability of tornadogenesis (e.g., Wicker 1996; Markowski and Richardson 2014; Markowski 2020; Coffer et al. 2017, 2023). Thus, supercells in large streamwise vorticity environments on average have more robust low-level mesocyclones (Flournoy et al. 2024).

While rotation of the mesocyclone is primarily due to the tilting of horizontal vorticity by an updraft, this process cannot produce vertical vorticity at surface¹ level because tilting requires the presence of an updraft gradient, so air parcels simultaneously rise away from the surface (Fig. 1a; Davies-Jones and Markowski 2013). In other words, tilting at this stage (in contrast to later during Stage 4) is not abrupt enough to cause appreciable near-surface vertical vorticity. Hence, pre-tornadic rotation arises through an entirely different set of processes.

Stage 2: Surface-level Rotation

While the mesocyclone is an important precursor to tornadogenesis, there also needs to be sufficient vertical vorticity at the surface from which the tornado can form. Vorticity is present all around us, manifesting in small structures such as the turbulent whirling of leaves behind obstacles on a windy day, to larger coherent structures in the atmospheric boundary layer (Young et al. 2002) and along airmass boundaries (e.g., Arnott et al. 2006; Marquis et al. 2007; Stonitsch and Markowski 2007). However, a mechanism that can consistently supply predominantly positive vertical vorticity beneath the low-level mesocyclone (see Fig. 1b) is likely to be the most supportive of tornadogenesis (Parker 2023). Different theoretical pathways exist to explain how vertical vorticity could be generated in such a systematic way (e.g., Davies-Jones 2015). In idealized supercell simulations, which are initialized without background vertical vorticity (see Markowski 2024, for recent indications how the story may be different *with* vertical vorticity in a turbulent boundary layer), the mechanism that has been shown to be most effective in facilitating consistent surface-level rotation in many studies is the *downdraft mechanism* (Davies-Jones and Brooks 1993), described as follows.

As illustrated in Fig. 1b, near-surface vertical vorticity forms on the periphery of any negatively-buoyant downdrafts through which air is moving horizontally. This is because a parcel of air travelling through the downdraft (black arrow) experiences a horizontal buoyancy gradient, which baroclinically generates horizontal vorticity (green vectors). This horizontal vorticity is then partially tilted into the vertical as the parcel approaches the surface (see e.g., Parker and Dahl 2015, for a detailed explanation). The general updraft-downdraft orientation in supercells (both downdrafts on the rear flank and the forward flank) is often such that predominantly positive vertical

¹Strictly speaking, the wind (and vertical vorticity) has to be zero exactly at the surface ($z=0$) so it would be more appropriate to speak of *near-surface* rotation here. However, to clearly distinguish rotation practically at the surface (Stage 2) from rotation aloft (Stage 1), we will use “surface” herein. This does not mean the vorticity is restricted to the surface. Some vertical extent is implied (see Fig. 1b,c).

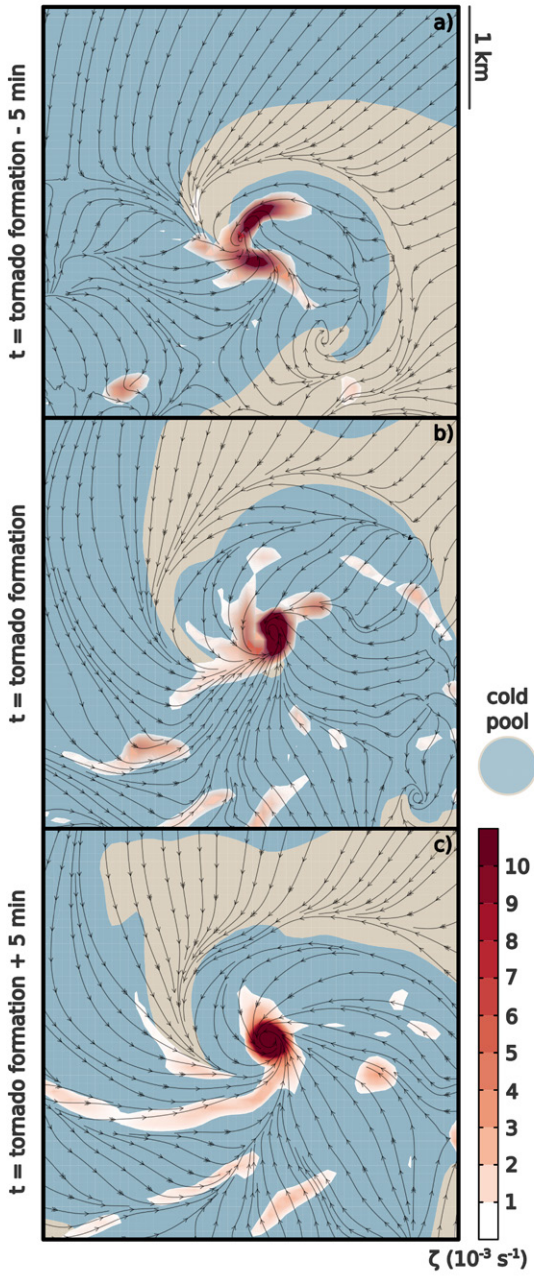


FIG. 2. An example of vortex patches evolving into a vortex from a high-resolution simulation ($\Delta x=80$ m) of a tornadic supercell from Coffer et al. (2023). Shown is the top down view of the cold pool shaded in blue, the vertical vorticity at 10 m above ground level (AGL) overlaid in red, and the horizontal streamlines at 10 m AGL at three times relative to tornado formation, (a) five minutes prior, (b) at tornado formation, (c) five minutes after. Tornado formation time was determined via vertical vorticity, pressure deficit, and wind speed thresholds.

vorticity builds up via this mechanism in the vicinity of the updraft (Markowski and Richardson 2014; Weiss et al. 2015; Fischer and Dahl 2020).

As shown in Fig. 2a, these areas with vertical vorticity in 2D are often elongated or amorphous in shape with several individual vorticity maxima in close proximity (Coffer et al. 2017; Orf et al. 2017). We will refer to these individual, pre-tornadic vertical vorticity maxima as *vortex patches* (the terms *vorticity rivers*, or *vortex sheets* are sometimes used synonymously depending on their size, shape and location). The scale of these vortex patches is diverse in simulations and, as discussed later on, observations of them have been sparse, so much uncertainty remains as to their true horizontal and vertical extent.

Regardless of the dimensions and origin, the simulated vortex patches initially tend to be weak and amorphous. They do not yet have the characteristics of a vortex (e.g., closed circular streamlines; Fig. 2a), which is essential for the characteristic structure of a tornado to develop as explained in Stage 3. Hence, tornado formation requires intensification (via stretching) *and* organization (to one symmetric vortex) of the vertical vorticity maxima.

Stage 3: Stretching and Organization

As already touched on in Stage 2 and shown in Fig. 2, high-resolution simulations suggest pre-tornadic vorticity first manifests in more complex structures than described in previous conceptual models (Davies-Jones 2015) and that these structures do not yet have vortical flow characteristics. Such a complex, nonuniform distribution of vertical vorticity tends to organize into a symmetric vortex over time simply via self-advection of the vorticity distribution by its own induced flow or due to the background flow (Dahl 2020; Figs. 1c and 2). In other words, elongated patches or sheets roll up (which is the same process operating during the release of shear instability; e.g., Rayleigh 1880; Gaudet and Cotton 2006; Gaudet et al. 2006; Dahl 2020) and individual vorticity maxima merge into a single, stronger maximum (Parker 2023). In supercells, this organization is sustained by the strong flow convergence near the ground because of the upward directed pressure gradient acceleration into the low-level mesocyclone. This convergence may be supported by the surging of the rear-flank outflow around the organizing rotation (Fig. 1c; e.g., Finley and Lee 2004). Additionally, the vertical acceleration leads to amplification of the vertical vorticity via stretching (hence the importance of low-level mesocyclone formation in Stage 1).

Both processes, organization and stretching, are necessary for an intense vortex to form. Acting against them are the negative buoyancy of the outflow (Markowski et al. 2002), horizontal advection of the developing vortex away from the optimal region below the mesocyclone (e.g., Dowell and Bluestein 2002; Fischer and Dahl 2023) and possible subsidence because of the decreasing pressure in the developing near-ground vortex causing a reversal of the vertical pressure gradient. Unfortunately, these factors are difficult to observe (e.g., outflow orientation, advection speed, temperature, and updraft velocities) and offer many possible tornadogenesis failure modes (e.g., Murdzek et al. 2020), which contributes to the low predictability of tornadoes (e.g., Markowski 2020). In the framework of our conceptual model it is sufficient to say that if the constructive factors above continuously dominate, an increasingly intense and symmetric vortex forms (Figs. 1c and 2b).

Stage 4: Transition

Throughout most of the vortex column resulting from Stage 3, the inward pressure gradient acceleration into the vortex core and the outward centrifugal acceleration are largely in balance horizontally (cyclostrophic balance). However, in the lowest few meters above the surface, known as the *tornado boundary layer*, a third acceleration becomes significant: surface drag. In this shallow layer, drag drastically decelerates the rotational velocity, which results in large inward-pointing horizontal vorticity in the tornado boundary layer. Furthermore, the retardation of the tangential flow by surface drag causes the centrifugal acceleration to weaken while the inward pressure gradient acceleration is unaffected.

As illustrated in Fig. 1d (see also the converging streamlines in Fig. 2b,c), the inward acceleration then causes the air to converge near the vortex core, where it erupts upward in a vertical jet. This dynamic response of the flow contributes to the extreme and damaging (vertical and horizontal) velocities near the ground, despite, or precisely because of, surface drag (Fiedler and Rotunno 1986; Lewellen 1993; Davies-Jones 2015). Since the flow direction rapidly turns from horizontal to mostly upward, this region is called the *corner flow*² (Lewellen 1976). As reviewed in detail by Rotunno (2013), laboratory and numerical experiments show the tornado boundary layer and

²The structure of the corner flow region is linked to the near-ground tornado structure (Lewellen et al. 2000; Lewellen and Lewellen 2007), which mainly varies between one-celled (with a swirling *end-wall jet* along the central axis) or two-celled (with a central downdraft and annular corner-flow region), as reviewed in Davies-Jones et al. (2001), Rotunno (2013), or Dahl (2021).

corner-flow region as characteristic features of fully-developed tornadoes. Hence, we can define tornadogenesis to be complete once a semi-steady vortex state with such features is established.

Importantly, air parcels now entering the tornado in this region develop vertical vorticity simply via abrupt upward tilting of their horizontal vorticity in the extreme velocity gradient of the corner flow region (Fig. 1d). This vertical vorticity source mechanism has long been recognized in fluid-dynamics studies of tornadoes (e.g., Rotunno 1980). Recently, it has received renewed attention in 3D supercell simulations and has been referred to as the *in-and-up* mechanism (Boyer and Dahl 2020; Fischer and Dahl 2022).

The transition to the in-and-up mechanism marks an important change in the dynamics because, for the tornado to persist, parcels entering the tornado now do not need to arrive with vertical vorticity, i.e., *the downdraft mechanism is not necessary anymore*. Only horizontal vorticity is required, which is typically large in the tornado boundary layer because of surface drag acting on the tornadic winds and because of the inward acceleration (Rotunno 2013; Fischer and Dahl 2023). In addition to surface drag, horizontal vorticity in the background environment or baroclinically generated horizontal vorticity can also be tilted in the corner flow region and thus may directly contribute to the tornado in the same way (Dahl and Fischer 2023). It is noteworthy that for studying tornadogenesis, identifying the timing of the transition is crucial (Fischer and Dahl 2023), because if one analyzes the process too late in their simulations or observations, one only finds the in-and-up mechanism as the source for tornadic rotation, not the mechanism which initially facilitated the tornado (Stage 2).

In short, the development of the tornado boundary layer and corner flow, and thus the tornado, hinges on the development of the intense pressure deficit that results from the axisymmetrization and stretching of the vertical vorticity extrema. Embedded in the supercell mesocyclone and updraft, the tornado then can theoretically persist unchanged, constantly generating and tilting its own vorticity as described above. In reality, external disruptive processes (e.g., Marquis et al. 2012) or a weakening mesocyclone eventually lead to the dissipation of the tornado.

Observations and Simulations of Tornadogenesis

Many of the discoveries and explanations above are predominantly based on computer simulations, in which individual storms can be studied in a controlled framework. Historically, owing

to limitations of computing power, modelers had to choose between simulating a storm in its entirety but with insufficient resolution to represent the tornado vortex (e.g., Wicker and Wilhelmson 1993), and performing high-resolution tornado-resolving simulations in smaller domains without the parent storm (e.g., Lewellen 1993). Thus, it was difficult to study tornado *genesis* within a thunderstorm using either type of simulation.

Today's computing power now allows for simulations of both the parent supercell storm and the tornado (e.g., Orf et al. 2017) and we have shown how much detail and complexity these recent simulations seem to reveal about tornadogenesis. However, many challenges remain. These include the parameterizations of microphysical processes (e.g., Dawson et al. 2010) and turbulence (Bryan et al. 2003; Markowski and Bryan 2016; Wang et al. 2020), which are flawed to different degrees, adding uncertainty to conclusions drawn from numerical simulations.

Hence, there often exists a disparity in conclusions across numerical modeling studies. In these situations, remote sensing and in-situ measurements of real storms are invaluable in establishing a consensus in the community. Do recent observations support the updated conceptual model presented herein?

A number of field campaigns have been dedicated to identifying sources of horizontal and vertical vorticity in supercell thunderstorms, attributable both to the ambient environment and the storm itself. The currently established model of tornadogenesis (Davies-Jones 2015) was largely built on observations from the VORTEX campaigns (Rasmussen et al. 1994; Wurman et al. 2012) in addition to pioneering simulation studies (e.g., Rotunno and Klemp 1985). More recently, a principal objective of the Targeted Observation by Radars and Unmanned Aircraft Systems (TORUS) project involved observation of the internal boundary regions of the supercell, focusing on the SVC, a region of intense streamwise horizontal vorticity feeding into the low-level mesocyclone (Fig. 3a,b; Orf et al. 2017; Schueth et al. 2021; Finley et al. 2023). Preliminary examination of a multitude of supercell forward flanks from TORUS indicates that SVCs exist in nature and can contribute to Stage 1 (i.e., to mesocyclonic rotation above the surface) but that they are by no means ubiquitous (Weiss and Schueth 2022).

Additionally, these extremely high-resolution mobile-radar observations seem to resolve individual vertical vorticity extrema with varying size (labelled as vortex sheets and patches in Fig. 3c,d; also see Dowell et al. 2002; Snyder et al. 2013). Hence, these observations suggest an even higher

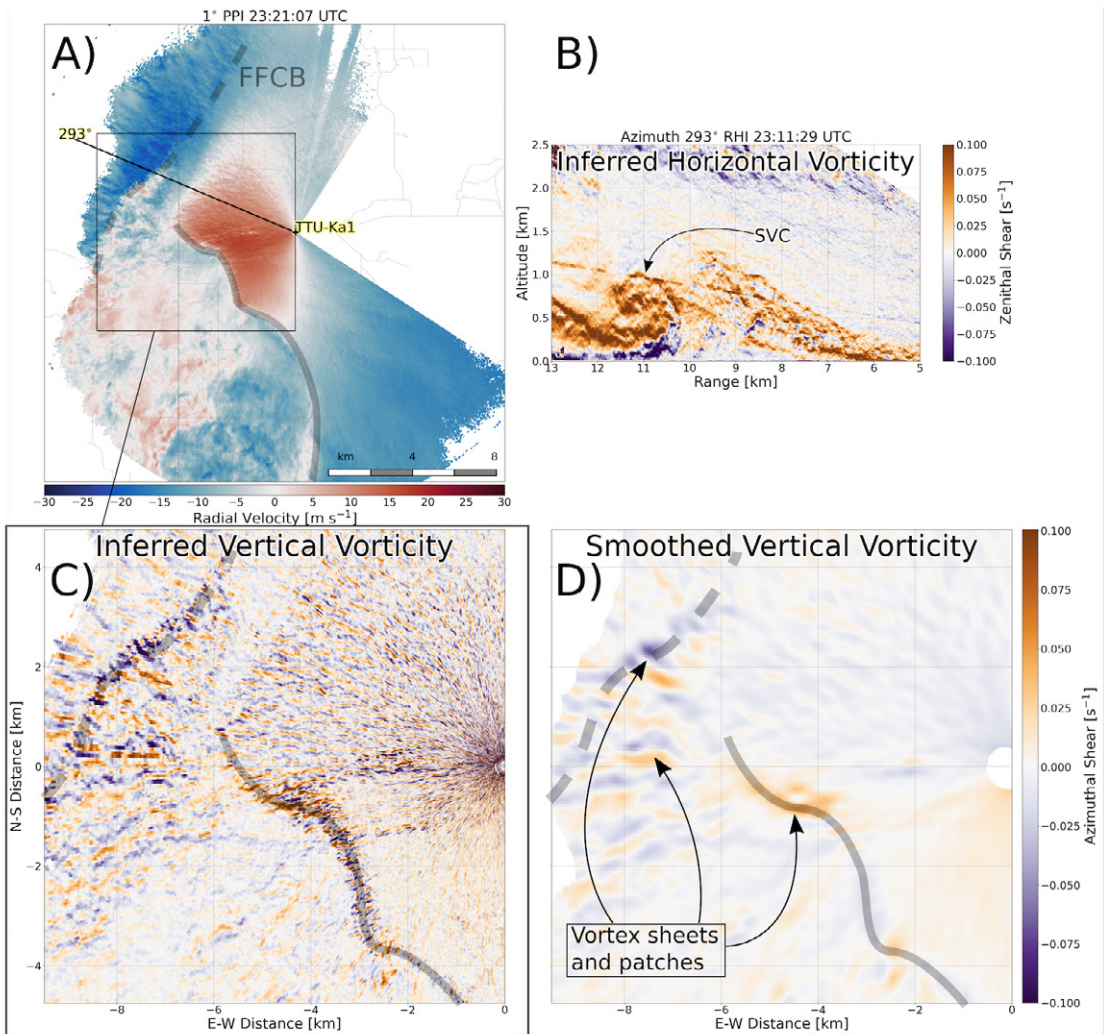


FIG. 3. Texas Tech Ka-band mobile Doppler radar scans of a supercell on 8 June 2018 23:21 UTC. (a) Radial velocity field at the lowest elevation angle (1°) for orientation of the mobile radar (TTU-Ka1) relative to the supercell to its west. The FFCB (Forward Flank Convergence Boundary) and RFGF (Rear Flank Gust Front) boundaries are indicated. (b) Vertical cross-section (RHI) through the FFCB at the location indicated in (a), 10 minutes earlier than (a), showing large horizontal vorticity, likely an SVC. (c) In a zoomed in part of (a), azimuthal shear, the radial component of vertical vorticity, is shown. (d) Same as (c) but smoothed using Barnes Analysis (Barnes 1964) on the radial velocity data before calculation of the azimuthal shear. Adapted from Schueth et al. (2021).

level of detail than most simulations (compare to Fig. 2) but they generally support the existence

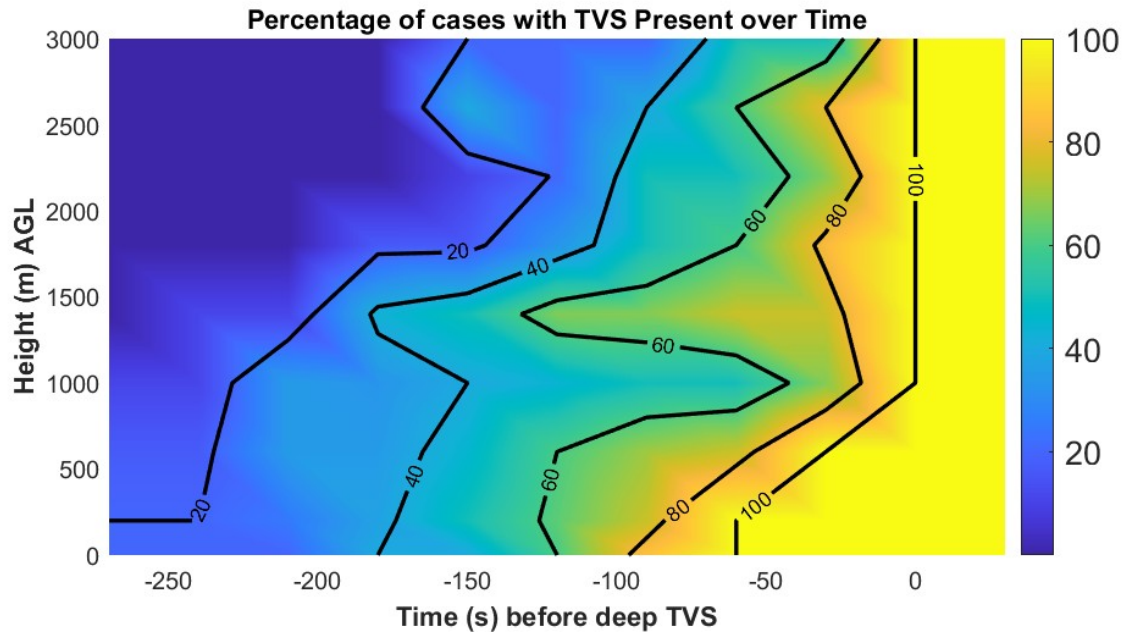


FIG. 4. Composite evolution of tornadogenesis based on 9 cases of Doppler radar observations. The contours show the percentage of cases which had a Tornadic Vortex Signature (TVS) at that time and height, with the cases synced to the first time at which a TVS was measured at all heights ($t = 0$). A TVS was defined as ΔV (difference between max inbound and max outbound radial velocities with distance D) $> 40 \text{ m s}^{-1}$ at a radius $< 1.5 \text{ km}$ and a gradient in $\Delta V > 40 \text{ m s}^{-1}$ per 250 m , or alternatively a $\Delta V > 35 \text{ m s}^{-1}$ with a pseudo vorticity $(2\Delta V/D) > 0.1 \text{ s}^{-1}$ (see Houser et al. 2015, 2022).

of vortex patch-like structures in the outflow of supercells (Step 2).³ More single and multiple-Doppler analyses with high spatio-temporal resolution of the near-ground wind field are required to establish the representativeness of this depiction.

Furthermore, recent studies with mobile Doppler radar observations of the 3D wind field with high temporal resolution successfully captured multiple tornadoes during genesis (French et al. 2013; Houser et al. 2015; Wienhoff et al. 2020; Houser et al. 2022). As shown in a composite of 9 cases in Fig. 4, radar-observed tornadic (or sub-tornadic) rotation tends to start at or very near the surface and builds upward with time, or it nearly simultaneously (within $\sim 1 \text{ min}$) intensifies to tornadic strength between the surface and the mesocyclone above. This is consistent with the

³As only the radial component of the wind can be measured by Doppler radar, inferred vertical vorticity (azimuthal shear) from single-Doppler radar analysis as in 3c,d can only resolve a component of the total vertical vorticity.

intensification and ingestion of surface vertical vorticity into the updraft (Stage 3) as well as the rapid intensification during transition to the in-and-up mechanism (Stage 4).

It is noteworthy that this radar-observed evolution of the wind field during tornadogenesis is often invisible to the human eye. A tornado's condensation funnel (Fig. SB1) only becomes visible once the vortex reaches a certain intensity. Hence, the funnel's *descent* over time provides a misleading impression of the actual *upward* tornado development (Fig. 4). This discrepancy is described in greater detail in the sidebar.

Summary and Where to Go from Here

Based on the published literature, we have updated the conceptual tornadogenesis model with four stages:

1. Mesocyclone formation, with the associated pressure perturbations driving upward acceleration and stretching near and below cloud base (critical for Stage 3)
2. Generation of vortex patches (amorphous surface-level vertical vorticity not yet with vortex characteristics), in simulations predominantly via reorientation of baroclinically generated vorticity in downdrafts
3. Organization of one or multiple vortex patches to a single symmetric vortex and intensification via stretching
4. Transition to a developed tornado with a vortex boundary layer and corner flow region in which horizontal vorticity is tilted into the vertical right above the surface

Recent observations support many of these findings from high-resolution simulations. Pre-tornadic vorticity first organizes and intensifies near the surface and then rapidly develops upward (Stage 3). However, the 3D evolution of these vortex patches is still uncertain. We see this as a key research topic where observations with high spatio-temporal resolution of near-ground supercell outflow could advance our understanding of tornadogenesis.

Many other open questions remain. How important are the SVC and surface roughness for low-level mesocyclone intensity in Stage 1? What processes, both of the supercell (mainly Stages 1-2) and of the vortex scale (mainly Stages 3-4), determine tornado size and intensity (e.g., Trapp et al. 2017; Markowski 2020)? How important are supercell-external factors not accounted for in

this conceptual model, such as storm mergers and mesoscale boundaries (e.g., Fischer and Dahl 2023) or turbulent eddies in the environmental boundary layer (Markowski 2024)?

It is also unclear whether this supercellular conceptual model applies to quasi-linear convective systems (QLCS), in which tornadoes are typically weaker than those forming in supercells, but may have a large impact in certain regions and seasons (Anderson-Frey and Brooks 2019). Some aspects of QLCS tornado formation are likely different from their supercell counterparts (e.g., Goodnight et al. 2022). However, vorticity organization and interaction of the developing vortex with the surface (Stages 3 and 4) are likely inevitable for any intense columnar vortex connected to the ground (probably including strong dust devils, gustnadoes, etc.).

As mentioned in Stage 1, some disagreement also exists in the analyses of supercell environments based on modeled or observed soundings. On the one hand, there are uncertainties associated with the representation of the near-ground wind profile in model analyses (Coniglio and Jewell 2021). On the other hand, many compilations of observed soundings have been under-dispersed in terms of season, region, and time of day, and have included primarily high-end supercells among their nontornadic cases. Future research is needed to address how the wind profile over varying layers influence important processes that potentially control tornado production, such as mesocyclone intensity and the distribution of hydrometeors, as well as to what degree model limitations may shade our impressions of what large near-ground streamwise vorticity hodographs really look like.

From the operational forecasting perspective, predicting which storms will become tornadic within a favorable environment is still extremely difficult (e.g., Brooks and Correia 2018). In light of the previous paragraph, forecasting and nowcasting of tornadoes could be improved with denser observations of the vertical wind profile (including emerging techniques discussed in Bell et al. 2020). Furthermore, continued focus on explaining the small-scale dynamics outlined herein provides the hope that eventually new pathways to tornado prediction and warning become possible. Research on all aspects of severe storms and on tornado dynamics will therefore continue to be of great societal interest.

Acknowledgments. Authors Dahl and Fischer worked on this topic under NSF grants AGS-1651786 and AGS-2152537. Authors Coffer and Parker are supported under NSF grant AGS-2130936, Weiss and Schueth under AGS-2312995, and Houser under AGS-1749504. Fischer is also currently a Willis Research Fellow. We thank Dr. Rich Rotunno for insightful discussions about tornado dynamics and Drs. M. Beyer, M. Kunz, S. Mohr, C. Nixon, J. Soderholm, and Mr. M. Tonn for their helpful comments on the manuscript.

Data availability statement. Data used in the studies reviewed herein is usually described in the respective publication. For specific questions, an email request can be sent to the corresponding author.

Sidebar 1: Does a tornado “touch down” or “spin up”? Funnel clouds (Fig. SB1), which build downward from the thunderstorm cloud, are often mistaken for a “descending” tornado. However, the time-height evolution of the funnel cloud is different than that of the tornado. In fact, during tornadogenesis the air is generally rising up into the updraft, not descending. As illustrated in Fig. SB2a, rising air encounters lower pressure with height, expands adiabatically, and thus cools down, until moisture saturation occurs at the lifted condensation level (LCL). In the absence of a tornado, the LCL therefore represents the base of the thunderstorm cloud. In spinning air (Fig. SB2b), centrifugal acceleration leads to a pressure deficit within the vortex (in addition to the decreasing pressure with height). The result is that the LCL is lowered and this locally lowered cloud base appears as the funnel cloud. When the vortex intensifies, the LCL (and funnel cloud) progressively descends to lower altitudes and can reach the ground. However, it is common to have tornadic winds at the surface and only a funnel aloft (Fig. SB1). In short, even though the funnel starts aloft and develops downward, the tornado itself is found in ascending air, and the rotation rate is usually similar throughout the whole column. The wind speeds may even be larger near ground level than near the funnel. Thus, a tornado does not touch down. It is more appropriate to say that the vortex organizes at the surface and *spins up* to tornadic intensity.



FIG. SB1. Example of a tornado with funnel cloud only in the upper half of the vortex. The surface winds were strong enough to whirl up dust and debris, which outline the lower half of the rotating column. Photo by M. Parker.

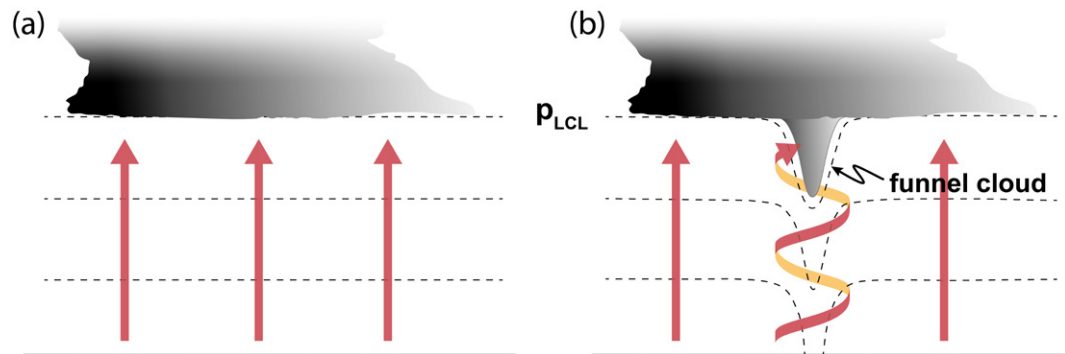


FIG. SB2. A schematic of funnel formation as explained in the text. A cloud base is illustrated in gray. (a) Rising air reaching saturation pressure (p_{LCL}) at cloud base. (b) Within a vortex (spiralling arrow), the saturation pressure is reached at lower altitudes, resulting in condensation at lower heights, i.e., a funnel. Gray lines indicate heights with equal pressure and red arrows that the air is mostly rising.

References

- Anderson-Frey, A. K., and H. Brooks, 2019: Tornado fatalities: An environmental perspective. *Wea. Forecasting*, **34** (6), 1999–2015, <https://doi.org/10.1175/WAF-D-19-0119.1>.
- Arnott, N. R., Y. P. Richardson, J. M. Wurman, and E. M. Rasmussen, 2006: Relationship between a weakening cold front, misocyclones, and cloud development on 10 june 2002 during ihop. *Mon. Wea. Rev.*, **134**, 311–335.
- Barnes, S. L., 1964: A Technique for Maximizing Details in Numerical Weather Map Analysis. *Journal of Applied Meteorology and Climatology*, **3** (4), 396–409, [https://doi.org/10.1175/1520-0450\(1964\)003<0396:ATFMDI>2.0.CO;2](https://doi.org/10.1175/1520-0450(1964)003<0396:ATFMDI>2.0.CO;2), URL https://journals.ametsoc.org/view/journals/apme/3/4/1520-0450_1964_003_0396_atfmdi_2_0_co_2.xml.
- Bell, T. M., B. R. Greene, P. M. Klein, M. Carney, and P. B. Chilson, 2020: Confronting the boundary layer data gap: evaluating new and existing methodologies of probing the lower atmosphere. *Atmospheric Measurement Techniques*, **13** (7), 3855–3872, <https://doi.org/10.5194/amt-13-3855-2020>, URL <https://amt.copernicus.org/articles/13/3855/2020/>.
- Boyer, C. H., and J. M. Dahl, 2020: The mechanisms responsible for large near-surface vertical vorticity within simulated supercells and quasi-linear storms. *Mon. Wea. Rev.*, **148** (10), 4281–4297, <https://doi.org/10.1175/MWR-D-20-0082.1>.
- Brooks, H. E., and J. Correia, 2018: Long-term performance metrics for National Weather Service Tornado warnings. *Wea. Forecasting*, **33** (6), 1501–1511, <https://doi.org/10.1175/WAF-D-18-0120.1>.
- Brotzge, J. A., S. E. Nelson, R. L. Thompson, and B. T. Smith, 2013: Tornado probability of detection and lead time as a function of convective mode and environmental parameters. *Weather and Forecasting*, **28** (5), 1261–1276, <https://doi.org/10.1175/WAF-D-12-00119.1>.
- Browning, K. A., 1962: The cellular structure of convective storms. *Meteor. Mag.*, **92**, 341–350.
- Bryan, G. H., J. C. Wyngaard, and J. M. Fritsch, 2003: Resolution requirements for the simulation of deep moist convection. *Monthly Weather Review*, **131** (10), 2394 – 2416, [https://doi.org/10.1175/1520-0493\(2003\)131<2394:RRFTSO>2.0.CO;2](https://doi.org/10.1175/1520-0493(2003)131<2394:RRFTSO>2.0.CO;2), URL https://journals.ametsoc.org/view/journals/mwre/131/10/1520-0493_2003_131_2394_rrftso_2.0.co_2.xml.

Coffer, B. E., and M. D. Parker, 2018: Is There a “Tipping Point” between Simulated Nontornadic and Tornadic Supercells in VORTEX2 Environments? *Mon. Wea. Rev.*, **146** (8), 2667–2693, <https://doi.org/10.1175/mwr-d-18-0050.1>.

Coffer, B. E., M. D. Parker, J. M. Dahl, L. J. Wicker, and A. J. Clark, 2017: Volatility of tornadogenesis: An ensemble of simulated nontornadic and tornadic supercells in VORTEX2 environments. *Mon. Wea. Rev.*, **145** (11), 4605–4625, <https://doi.org/10.1175/MWR-D-17-0152.1>.

Coffer, B. E., M. D. Parker, J. M. Peters, and A. R. Wade, 2023: Supercell low-level mesocyclones: Origins of inflow and vorticity. *Monthly Weather Review*, <https://doi.org/https://doi.org/10.1175/MWR-D-22-0269.1>, URL <https://journals.ametsoc.org/view/journals/mwre/aop/MWR-D-22-0269.1/MWR-D-22-0269.1.xml>.

Coffer, B. E., M. D. Parker, R. L. Thompson, B. T. Smith, and R. E. Jewell, 2019: Using near-ground storm relative helicity in supercell tornado forecasting. *Weather and Forecasting*, **34** (5), 1417–1435.

Coffer, B. E., M. Taszarek, and M. D. Parker, 2020: Near-ground wind profiles of tornadic and nontornadic environments in the United States and Europe from ERA5 reanalyses. *Wea. Forecasting*, 1–52, <https://doi.org/10.1175/waf-d-20-0153.1>.

Coniglio, M. C., and R. E. Jewell, 2021: SPC Mesoscale Analysis Compared to Field-Project Soundings: Implications for Supercell Environment Studies. *Monthly Weather Review*, <https://doi.org/10.1175/MWR-D-21-0222.1>, URL <https://journals.ametsoc.org/view/journals/mwre/aop/MWR-D-21-0222.1/MWR-D-21-0222.1.xml>.

Coniglio, M. C., and M. D. Parker, 2020: Insights into supercells and their environments from three decades of targeted radiosonde observations. *Mon. Wea. Rev.*, **148**, 4893–4916, <https://doi.org/10.1175/mwr-d-20-0105.1>.

Craven, J. P., and H. E. Brooks, 2004: Baseline climatology of sounding derived parameters associated with deep, moist convection. *National Weather Digest*, **28**, 13–24.

Dahl, J. M., 2021: Centrifugal waves in tornado-like vortices: Kelvin's solutions and their applications to multiple-vortex development and vortex breakdown. *Mon. Wea. Rev.*, **149** (10), 3173–3216, <https://doi.org/10.1175/MWR-D-20-0426.1>.

Dahl, J. M. L., 2017: Tilting of Horizontal Shear Vorticity and the Development of Updraft Rotation in Supercell Thunderstorms. *J. Atmos. Sci.*, **74** (9), 2997–3020, <https://doi.org/10.1175/jas-d-17-0091.1>.

Dahl, J. M. L., 2020: Near-Surface Vortex Formation in Supercells from the Perspective of Vortex Patch Dynamics. *Mon. Wea. Rev.*, **148** (8), 3533–3547, <https://doi.org/10.1175/MWR-D-20-0080.1>.

Dahl, J. M. L., and J. Fischer, 2023: On the Origins of Vorticity in a Simulated Tornado-Like Vortex. *Journal of the Atmospheric Sciences*, [https://doi.org/https://doi.org/10.1175/JAS-D-22-0145.1](https://doi.org/10.1175/JAS-D-22-0145.1), URL <https://journals.ametsoc.org/view/journals/atsc/aop/JAS-D-22-0145.1/JAS-D-22-0145.1.xml>.

Davies-Jones, R., 1984: Streamwise Vorticity: The Origin of Updraft Rotation in Supercell Storms. *J. Atmos. Sci.*, **41** (20), 2991–3006.

Davies-Jones, R., 2015: A review of supercell and tornado dynamics. *Atmos. Res.*, **158-159**, 274–291, <https://doi.org/10.1016/j.atmosres.2014.04.007>.

Davies-Jones, R., and H. Brooks, 1993: Mesocyclogenesis from a Theoretical Perspective. *The Tornado: Its Structure, Dynamics, Prediction, and Hazards*, **79**, 105–114.

Davies-Jones, R., and P. Markowski, 2013: Lifting of ambient air by density currents in sheared environments. *J. Atmos. Sci.*, **70** (4), 1204–1215, <https://doi.org/10.1175/JAS-D-12-0149.1>.

Davies-Jones, R., R. J. Trapp, and H. B. Bluestein, 2001: Tornadoes and Tornadic Storms. *Meteorological Monographs*, **50** (November), 167–222, <https://doi.org/10.1175/0065-9401-28.50.167>.

Dawson, D. T., M. Xue, J. A. Milbrandt, and M. K. Yau, 2010: Comparison of evaporation and cold pool development between single-moment and multimoment bulk microphysics schemes in idealized simulations of tornadic thunderstorms. *Monthly Weather Review*, **138** (4), 1152 –

1171, <https://doi.org/https://doi.org/10.1175/2009MWR2956.1>, URL <https://journals.ametsoc.org/view/journals/mwre/138/4/2009mwr2956.1.xml>.

Doswell, C. A., and D. W. Burgess, 1993: *Tornadoes and Tornadic Storms: a Review of Conceptual Models*, 161–172. American Geophysical Union (AGU), <https://doi.org/https://doi.org/10.1029/GM079p0161>.

Dowell, D. C., and H. B. Bluestein, 2002: The 8 june 1995 mclean, texas, storm. part ii: Cyclic tornado formation, maintenance, and dissipation. *Monthly Weather Review*, **130**, 2649–2670, [https://doi.org/10.1175/1520-0493\(2002\)130<2649:TJMTSP>2.0.CO;2](https://doi.org/10.1175/1520-0493(2002)130<2649:TJMTSP>2.0.CO;2).

Dowell, D. C., Y. P. Richardson, and J. M. Wurman, 2002: Observations of the formation of low-level rotation: The 5 june 2001 sumner county, kansas storm. *21st AMS Conference on Severe Local Storms*, URL <https://api.semanticscholar.org/CorpusID:209321449>.

Fiedler, B. H., and R. Rotunno, 1986: A theory for the maximum windspeeds in tornado-like vortices. *J. Atmos. Sci.*, **43**, 2328–2340.

Finley, C. A., M. Elmore, L. Orf, and B. D. Lee, 2023: Impact of the streamwise vorticity current on low-level mesocyclone development in a simulated supercell. *Geophysical Research Letters*, **50** (1), e2022GL100 005.

Finley, C. A., and B. D. Lee, 2004: High Resolution Mobile Mesonet Observations of Rfd Surges in the June 9 Basset , Nebraska Supercell During Project Answers 2003. *22nd AMS Conference on Severe Local Storms*.

Fischer, J., and J. M. Dahl, 2022: Transition of Near-Ground Vorticity Dynamics During Tornadogenesis. *J. Atmos. Sci.*, **79**, 467–483, <https://doi.org/10.1175/jas-d-21-0181.1>.

Fischer, J., and J. M. L. Dahl, 2020: The Relative Importance of Updraft and Cold Pool Characteristics in Supercell Tornadogenesis Using Highly Idealized Simulations. *J. Atmos. Sci.*, **77** (12), 4089–4107, <https://doi.org/10.1175/jas-d-20-0126.1>.

Fischer, J., and J. M. L. Dahl, 2023: Supercell-External Storms and Boundaries acting as Catalysts for Tornadogenesis. *Monthly Weather Review*, 23–38, <https://doi.org/10.1175/mwr-d-22-0026.1>.

French, M. M., H. B. Bluestein, I. Popstefanija, C. A. Baldi, and R. T. Bluth, 2013: Reexamining the vertical development of tornadic vortex signatures in supercells. *Mon. Wea. Rev.*, **141** (12), 4576–4601, <https://doi.org/10.1175/MWR-D-12-00315.1>.

Gaudet, B. J., and W. R. Cotton, 2006: Low-level mesocyclonic concentration by nonaxisymmetric transport. Part I: Supercell and mesocyclone evolution. *J. Atmos. Sci.*, **63** (4), 1113–1133, <https://doi.org/10.1175/JAS3685.1>.

Gaudet, B. J., W. R. Cotton, and M. T. Montgomery, 2006: Low-level mesocyclonic concentration by nonaxisymmetric transport. Part II: Vorticity dynamics. *J. Atmos. Sci.*, **63** (4), 1134–1150, <https://doi.org/10.1175/JAS3579.1>.

Goldacker, N. A., and M. D. Parker, 2021: Low-level updraft intensification in response to environmental wind profiles. *Journal of the Atmospheric Sciences*, **78** (9), 2763–2781.

Goodnight, J. S., D. A. Chehak, and R. J. Trapp, 2022: Quantification of qlcs tornadogenesis, associated characteristics, and environments across a large sample. *Weather and Forecasting*, **37** (11), 2087–2105, <https://doi.org/10.1175/WAF-D-22-0016.1>, URL <https://journals.ametsoc.org/view/journals/wefo/37/11/WAF-D-22-0016.1.xml>.

Houser, J. L., H. B. Bluestein, and J. C. Snyder, 2015: Rapid-scan, polarimetric, doppler radar observations of tornadogenesis and tornado dissipation in a tornadic supercell: The "El Reno, Oklahoma" storm of 24 May 2011. *Mon. Wea. Rev.*, **143** (7), 2685–2710, <https://doi.org/10.1175/MWR-D-14-00253.1>.

Houser, J. L., H. B. Bluestein, K. Thiem, J. Snyder, D. Reif, and Z. Wienhoff, 2022: Additional Evaluation of the Spatiotemporal Evolution of Rotation during Tornadogenesis Using Rapid-Scan Mobile Radar Observations. *Monthly Weather Review*, **150** (7), 1639–1666, <https://doi.org/10.1175/MWR-D-21-0227.1>.

Klemp, J. B., and R. Rotunno, 1983: A study of the tornadic region within a supercell thunderstorm. *Journal of Atmospheric Sciences*, **40** (2), 359 – 377, [https://doi.org/10.1175/1520-0469\(1983\)040<0359:ASOTTR>2.0.CO;2](https://doi.org/10.1175/1520-0469(1983)040<0359:ASOTTR>2.0.CO;2), URL https://journals.ametsoc.org/view/journals/atsc/40/2/1520-0469_1983_040_0359_asottr_2_0_co_2.xml.

Lewellen, D. C., and W. S. Lewellen, 2007: Near-surface intensification of tornado vortices. *J. Atmos. Sci.*, **64** (7), 2176–2194, <https://doi.org/10.1175/JAS3965.1>.

Lewellen, D. C., W. S. Lewellen, and J. Xia, 2000: The influence of a local swirl ratio on tornado intensification near the surface. *J. Atmos. Sci.*, **57** (4), 527–544, [https://doi.org/10.1175/1520-0469\(2000\)057<0527:TIOALS>2.0.CO;2](https://doi.org/10.1175/1520-0469(2000)057<0527:TIOALS>2.0.CO;2).

Lewellen, W. S., 1976: Assessment of knowledge and implications for man. *Proc. Symp. on Tornadoes*, Texas Tech University, Lubbock, TX, 107–143.

Lewellen, W. S., 1993: Tornado Vortex Theory. *The Tornado: Its Structure, Dynamics, Prediction, and Hazards*, **79**, 19–39.

Lilly, D. K., 1982: The development and maintenance of rotation in convective storms. *Intense Atmospheric Vortices*, L. Bengtsson, and J. Lighthill, Eds., Springer Berlin Heidelberg, Berlin, Heidelberg, 149–160.

Markowski, P., C. Hannon, J. Frame, E. Lancaster, A. Pietrycha, R. Edwards, and R. L. Thompson, 2003: Characteristics of vertical wind profiles near supercells obtained from the rapid update cycle. *Weather and forecasting*, **18** (6), 1262–1272.

Markowski, P., and Y. Richardson, 2010: *Mesoscale meteorology in midlatitudes*, Vol. 2. John Wiley and Sons.

Markowski, P., and Coauthors, 2012: The pretornadic phase of the Goshen County, Wyoming, supercell of 5 June 2009 intercepted by VORTEX2. Part II: Intensification of low-level rotation. *Monthly weather review*, **140** (9), 2916–2938.

Markowski, P. M., 2020: What is the intrinsic predictability of tornadic supercell thunderstorms? *Mon. Wea. Rev.*, **148** (8), 3157–3180, <https://doi.org/10.1175/mwr-d-20-0076.1>.

Markowski, P. M., 2024: A New Pathway for Tornadogenesis Exposed by Numerical Simulations of Supercells in Turbulent Environments. *Journal of the Atmospheric Sciences*, **81** (3), 481–518, <https://doi.org/10.1175/JAS-D-23-0161.1>.

Markowski, P. M., and G. H. Bryan, 2016: LES of Laminar Flow in the PBL: A Potential Problem for Convective Storm Simulations. *Mon. Wea. Rev.*, **144** (5), 1841–1850, <https://doi.org/10.1175/mwr-d-15-0439.1>.

Markowski, P. M., and Y. P. Richardson, 2014: The Influence of Environmental Low-Level Shear and Cold Pools on Tornadogenesis: Insights from Idealized Simulations. *J. Atmos. Sci.*, **71** (1), 243–275, <https://doi.org/10.1175/jas-d-13-0159.1>.

Markowski, P. M., J. M. Straka, and E. N. Rasmussen, 2002: Direct surface thermodynamic observations within the rear-flank downdrafts of nontornadic and tornadic supercells. *Mon. Wea. Rev.*, **130** (7), 1692–1721, [https://doi.org/10.1175/1520-0493\(2002\)130<1692:DSTOWT>2.0.CO;2](https://doi.org/10.1175/1520-0493(2002)130<1692:DSTOWT>2.0.CO;2).

Marquis, J., Y. Richardson, P. Markowski, D. Dowell, and J. Wurman, 2012: Tornado maintenance investigated with high-resolution dual-doppler and enkf analysis. *Monthly Weather Review*, **140** (1), 3 – 27, <https://doi.org/10.1175/MWR-D-11-00025.1>, URL <https://journals.ametsoc.org/view/journals/mwre/140/1/mwr-d-11-00025.1.xml>.

Marquis, J., Y. P. Richardson, and J. M. Wurman, 2007: Kinematic observations of misocyclones along boundaries during ihop. *Mon. Wea. Rev.*, **135**, 1749–1768.

Murdzek, S. S., P. M. Markowski, Y. P. Richardson, and R. L. Tanamachi, 2020: Processes preventing the development of a significant tornado in a Colorado supercell on 26 May 2010. *Mon. Wea. Rev.*, **148** (5), 1753–1778, <https://doi.org/10.1175/MWR-D-19-0288.1>.

Nixon, C. J., and J. T. Allen, 2022: Distinguishing between Hodographs of Severe Hail and Tornadoes. *Weather and Forecasting*, **37** (10), 1761–1782, <https://doi.org/10.1175/WAF-D-21-0136.1>.

Orf, L., R. Wilhelmson, B. Lee, C. Finley, and A. Houston, 2017: Evolution of a long-track violent tornado within a simulated supercell. *Bull. Amer. Meteor. Soc.*, **98** (1), 45–68, <https://doi.org/10.1175/BAMS-D-15-00073.1>.

Parker, M. D., 2014: Composite VORTEX2 supercell environments from near-storm soundings. *Mon. Wea. Rev.*, **142** (2), 508–529, <https://doi.org/10.1175/MWR-D-13-00167.1>.

Parker, M. D., 2023: How well must surface vorticity be organized for tornadogenesis? *Journal of the Atmospheric Sciences*, [https://doi.org/https://doi.org/10.1175/JAS-D-22-0195.1](https://doi.org/10.1175/JAS-D-22-0195.1), URL <https://journals.ametsoc.org/view/journals/atsc/aop/JAS-D-22-0195.1/JAS-D-22-0195.1.xml>.

Parker, M. D., and J. M. L. Dahl, 2015: Production of Near-Surface Vertical Vorticity by Idealized Downdrafts. *Mon. Wea. Rev.*, **143** (7), 2795–2816, <https://doi.org/10.1175/mwr-d-14-00310.1>.

Peters, J. M., B. E. Coffer, M. D. Parker, C. J. Nowotarski, J. P. Mulholland, C. J. Nixon, and J. T. Allen, 2023: Disentangling the influences of storm-relative flow and horizontal streamwise vorticity on low-level mesocyclones in supercells. *Journal of the Atmospheric Sciences*, 129–149, <https://doi.org/10.1175/jas-d-22-0114.1>.

Rasmussen, E. N., 2003: Refined supercell and tornado forecast parameters. *Weather and Forecasting*, **18** (3), 530–535.

Rasmussen, E. N., J. M. Straka, R. Davies-Jones, C. A. Doswell, F. H. Carr, M. D. Eilts, and D. R. MacGorman, 1994: Verification of the origins of rotation in tornadoes experiment: Vortex. *Bulletin of the American Meteorological Society*, **75** (6), 995 – 1006, [https://doi.org/https://doi.org/10.1175/1520-0477\(1994\)075<995:VOTOOR>2.0.CO;2](https://doi.org/10.1175/1520-0477(1994)075<995:VOTOOR>2.0.CO;2), URL https://journals.ametsoc.org/view/journals/bams/75/6/1520-0477_1994_075_0995_votoor_2_0_co_2.xml.

Rayleigh, L., 1880: On the Stability, or Instability, of certain Fluid Motions. *Proceedings of the London Mathematical Society*, **s1-11** (1), 57–72, <https://doi.org/10.1112/plms/s1-11.1.57>, URL <https://doi.org/10.1112/plms/s1-11.1.57>.

Roberts, B., and M. Xue, 2017: The role of surface drag in mesocyclone intensification leading to tornadogenesis within an idealized supercell simulation. *J. Atmos. Sci.*, **74** (9), 3055–3077, <https://doi.org/10.1175/JAS-D-16-0364.1>.

Rotunno, R., 1980: Vorticity dynamics of a convective swirling boundary layer. *Journal of Fluid Mechanics*, **97** (3), 623–640, <https://doi.org/10.1017/S0022112080002728>.

Rotunno, R., 1981: On the evolution of thunderstorm rotation. *Monthly Weather Review*, **109** (3), 577–586.

Rotunno, R., 1993: *Supercell Thunderstorm Modeling and Theory*, 57–73. American Geophysical Union (AGU), [https://doi.org/https://doi.org/10.1029/GM079p0057](https://doi.org/10.1029/GM079p0057), URL <https://doi.org/https://doi.org/10.1029/GM079p0057>.

agupubs.onlinelibrary.wiley.com/doi/abs/10.1029/GM079p0057, <https://agupubs.onlinelibrary.wiley.com/doi/pdf/10.1029/GM079p0057>.

Rotunno, R., 2013: The Fluid Dynamics of Tornadoes. *Annu. Rev. Fluid Mech.*, **45** (1), 59–84, <https://doi.org/10.1146/annurev-fluid-011212-140639>.

Rotunno, R., and J. B. Klemp, 1985: On the rotation and propagation of simulated supercell thunderstorms. *J. Atmos. Sci.*, **42** (3), 271–292, [https://doi.org/10.1175/1520-0469\(1985\)042<0271:OTRAPO>2.0.CO;2](https://doi.org/10.1175/1520-0469(1985)042<0271:OTRAPO>2.0.CO;2).

Schueth, A., C. Weiss, and J. M. Dahl, 2021: Comparing Observations and Simulations of the Streamwise Vorticity Current and the Forward Flank Convergence Boundary in a Supercell Storm. *Mon. Wea. Rev.*, **149**, 1651–1671, <https://doi.org/10.1175/mwr-d-20-0251.1>.

Schultz, D. M., Y. P. Richardson, P. M. Markowski, and C. A. Doswell, 2014: Tornadoes in the Central United States and the "clash of air masses". *Bulletin of the American Meteorological Society*, **95** (11), 1704–1712, <https://doi.org/10.1175/BAMS-D-13-00252.1>.

Snyder, J. C., H. B. Bluestein, V. Venkatesh, and S. J. Frasier, 2013: Observations of polarimetric signatures in supercells by an x-band mobile doppler radar. *Monthly Weather Review*, **141** (1), 3–29, <https://doi.org/10.1175/MWR-D-12-00068.1>, URL <https://journals.ametsoc.org/view/journals/mwre/141/1/mwr-d-12-00068.1.xml>.

Stonitsch, J. R., and P. M. Markowski, 2007: Unusually long duration, multiple-doppler radar observations of front in a convective boundary layer. *Monthly Weather Review*, **135** (1), 93–117, <https://doi.org/10.1175/MWR3261.1>.

Thompson, R. L., B. T. Smith, J. S. Grams, A. R. Dean, and C. Broyles, 2012: Convective modes for significant severe thunderstorms in the contiguous United States. Part II: Supercell and QLCS tornado environments. *Weather and Forecasting*, **27** (5), 1136–1154, <https://doi.org/10.1175/WAF-D-11-00116.1>.

Thompson, R. L., and Coauthors, 2017: Tornado damage rating probabilities derived from WSR-88D data. *Weather and Forecasting*, **32** (4), 1509–1528.

Trapp, R. J., G. R. Marion, and S. W. Nesbitt, 2017: The regulation of tornado intensity by updraft width. *J. Atmos. Sci.*, **74** (12), 4199–4211, <https://doi.org/10.1175/JAS-D-16-0331.1>.

Wang, A., Y. Pan, and P. M. Markowski, 2020: The influence of turbulence memory on idealized tornado simulations. *Mon. Wea. Rev.*, **148** (12), 4875–4892, <https://doi.org/10.1175/MWR-D-20-0031.1>.

Weisman, M. L., and J. B. Klemp, 1984: The structure and classification of numerically simulated convective storms in directionally varying wind shears. *Monthly weather review*, **112** (12), 2479–2498.

Weiss, C. C., D. C. Dowell, J. L. Schroeder, P. S. Skinner, A. E. Reinhart, P. M. Markowski, and Y. P. Richardson, 2015: A comparison of near-surface buoyancy and baroclinity across three VORTEX2 supercell intercepts. *Mon. Wea. Rev.*, **143** (7), 2736–2753, <https://doi.org/10.1175/MWR-D-14-00307.1>.

Weiss, C. C., and A. Schueth, 2022: The kinematic character of forward flank outflows from the torus project. *30th Conference on Severe Local Storms.*, Paper 5.3.

Wicker, L. J., 1996: The role of near surface wind shear on low-level mesocyclone generation and tornadoes. *Preprints, 18th Conf. on Severe Local Storms, San Francisco, CA, Amer. Meteor. Soc.*, Vol. 115, 119.

Wicker, L. J., and R. B. Wilhelmson, 1993: Numerical Simulation of Tornadogenesis Within a Supercell Thunderstorm. *The Tornado: Its Structure, Dynamics, Prediction, and Hazards*, **79**, 75–88.

Wienhoff, Z. B., H. B. Bluestein, D. W. Reif, R. M. Wakimoto, L. J. Wicker, and J. M. Kurdzo, 2020: Analysis of debris signature characteristics and evolution in the 24 may 2016 dodge city, kansas, tornadoes. *Monthly Weather Review*, **148** (12), 5063–5086, <https://doi.org/10.1175/MWR-D-20-0162.1>, URL <https://journals.ametsoc.org/view/journals/mwre/148/12/mwr-d-20-0162.1.xml>.

Wurman, J., D. Dowell, Y. Richardson, P. Markowski, E. Rasmussen, D. Burgess, L. Wicker, and H. B. Bluestein, 2012: The second verification of the origins of rotation in tornadoes experiment: Vortex2. *Bulletin of the American Meteorological Society*, **93** (8), 1147 – 1170, <https://doi.org/https://doi.org/10.1175/BAMS-D-11-00010.1>, URL <https://journals.ametsoc.org/view/journals/bams/93/8/bams-d-11-00010.1.xml>.

Young, G. S., D. A. R. Kristovich, M. R. Hjelmfelt, and R. C. Foster, 2002: Rolls, streets, waves, and more: A review of quasi-two-dimensional structures in the atmospheric boundary layer. *Bulletin of the American Meteorological Society*, **83** (7), 997 – 1002, [https://doi.org/https://doi.org/10.1175/1520-0477\(2002\)083\(0997:RSWAMA\)2.3.CO;2](https://doi.org/https://doi.org/10.1175/1520-0477(2002)083(0997:RSWAMA)2.3.CO;2), URL https://journals.ametsoc.org/view/journals/bams/83/7/1520-0477_2002_083_0997_rswama_2_3_co_2.xml.